Available online at www.sciencedirect.com
ScienceDirect
Measurement 41 (2008) 105–118
Measurement
www.elsevier.com/locate/measurement

Higher-order spectra measurement techniques of termite emissions. A characterization framework ☆

Juan José González de la Rosa [a,*], I. Lloret [a], C.G. Puntonet [b], R. Piotrkowski [c], A. Moreno [d]

[a] University of Cádiz, Electronics Area, Research Group PAI-TIC-168: Computational Instrumentation and Industrial Electronics, EPSA, Avda. Ramón Puyol S/N, E-11202, Algeciras, Cádiz, Spain
[b] University of Granada, Department of Architecture and Computers Technology, ESII, C/Periodista Daniel Saucedo, E-18071 Granada, Spain
[c] Comisión Nacional de Energía Atómica-Univ, Nacional de General San Martín, Avda. General Paz. 1499, E-1650 San Martín-Buenos Aires, Argentina
[d] University of Córdoba, Electronics Area, Research Group PAI-TIC-168: Computational Instrumentation and Industrial Electronics, Campus de Rabanales, A. Einstein C-2, E-14071 Córdoba, Spain

Received 3 June 2005; accepted 3 October 2006
Available online 13 October 2006

Abstract

A higher-order frequency-domain characterization of termite activity (feeding and excavating) has been performed by means of analyzing diagonal slices of the bispectrum and the trispectrum, with the main goal of reducing subjectiveness in the task of detecting a possible infestation in a noisy measurement scenario. Five sets of signals of different qualities were acquired using two different accelerometers: an insect-oriented model and a seismic-waves sensor. We conclude that it is possible to establish a higher-order pattern associated to the termite emissions, and resulting from the impulsive response of the sensor and the body or substratum through which the emitted waves propagate.

Keywords: Accelerometer; Acoustic emission; Autocumulant; Bispectrum; Cumulants; Noisy readings; Termite detection; Transient characterization; Trispectrum; Ultrasonics; Vibratory signals

1. Introduction

Termite detection has been gaining importance in the last decade mainly due to the urgent necessity of avoiding the use of harming termiticides, and to the joint use of new emerging techniques of detection and hormonal treatments, with the aim of performing an early treatment of the infestation. A localized partial infestation can be exterminated after two or three generations of these insects with the aid of

* This work has been funded by the Spanish Ministry of Education and Science in the frame of the projects PTR1995-0824-OP and DPI2003-00878, and by the Andalusian Government via the project TIC155.
* Corresponding author. Tel.: +34 956028020; fax: +34 956028001.
E-mail address: juanjose.delarosa@uca.es (J.J. González de la Rosa).

0263-2241/$ - see front matter © 2006 Elsevier Ltd. All rights reserved.
doi:10.1016/j.measurement.2006.10.002

hormones. *Workers* stop feeding the *queen* termite of the colony, which dies of starvation, finishing the reproduction process, and consequently cutting any possible replacement of the members of the colony with a new generation.

The primary method of termite detection consists of looking for evidence of activity. But only about 25% of the building structure is accessible, and the conclusions depend very much on the level of expertise and the criteria of the inspector [1]. As a consequence, new techniques have been developed to remove subjectiveness and gain accessibility.

User-friendly equipment is being currently used in targeting subterranean insect infestations by means of temporal analysis of the vibratory data sequences.[1] An acoustic-emission (AE) sensor or an accelerometer is fixed to the suspicious structure. Counting the hits produced by the insects and being registered by the accelerometer; the instrument outputs light signals. At the same time, the user can listen to the sounds and perform some pre-processing, like filtering or amplifying. A set of hits is defined as an acoustic event, which in fact constitute the electronic *tracks* of these insects.

This class of instruments are based on the calculation of the root mean square (RMS) value of the vibratory waveform. This RMS value comprises information of the AE raw signal power during each interval of measurement, reducing the dynamic range and, consequently, leading to a loss of potentially valuable information. The use of the RMS value can be understood both by the difficulty of working in the high-frequency range of raw AE sequences, and by the lack of understanding of AE waves sources and propagation. Noisy media and anisotropy makes even harder the implementation of new methods of calculation and measurement procedures.

A more sophisticated family of instruments make use of spectral analysis and digital filtering to detect and characterize vibratory signals [2]. Both classes of systems (counting-assemblies and spectrum-based) have the drawback of the relative high cost and their practical limitations.

In fact, the usefulness of the above prior-art acoustic techniques and equipment for detection depends very much on several biophysical factors. The main one is the amount of distortion and attenuation as the sound travels through the soil ($\sim$600 dB m^{-1}, compared with 0.008 dB m^{-1} in the air). Furthermore, soil and wood are far from being ideal vibratory propagation media because of their high anisotropy and frequency dependent attenuation characteristics [2]. This is the reason whereby digital signal processing techniques emerged as an alternative.

On the other hand, second order statistics (i.e. correlation and power spectra estimation, the second order spectrum) failure in low SNR conditions, even with *ad hoc* piezoelectric sensors. Spectrum estimation and spectrogram extract time–frequency features, but ignoring phase properties of the signals. Besides, second-order algorithms are very sensitive to noise, which makes the users' identification criteria (mainly based on frequency-pattern recognition) being difficult to apply without great uncertainty.

Other prior-art second-order tools, like wavelets and wavelet packets (time-dependent technique) concentrate on transients and non-stationary movements, making possible the detection of singularities and sharp transitions, by means of subband decomposition. The method has been proved under controlled laboratory conditions, up to a SNR $= -30$ dB [3].

Higher-Order Statistics (HOS), like the bispectrum, have proven to be a useful tool for characterization of termites' emissions, using a synthetics of termite alarms and prior-known symmetrically distributed noise processes [4,5]. Cumulants have been modelled in order to characterize propagation of ultrasound in materials [6]. Other HOS tools, like the bicepstrum, have been successfully used in blind identification of acoustic emissions [7]. The conclusions of these works were funded in the advantages of cumulants; in particular, in the capability of enhancing the SNR of a signal buried in symmetrically distributed noise processes. The computational cost could be pointed out as the main drawback of the technique. Besides, in the practice, the goal is to localize the infestation from weak evidences, in order to prevent greater destruction. For that reason it should be emphasized that non-audible signals have to be detected.

In this paper we use higher-order spectra slices to characterize termite emissions. We present a set of graphical materials which help the researcher on HOS understand the interpretation of higher-order frequency diagrams; in particular in the field of insect characterization by AE signal processing. The con-

[1] The system AED-2000 (Acoustic Emission Consulting) has proven to be an advance in the detection of several insect species.

clusions are based in records which were acquired in several locations within the surrounding perimeter of the infestation. The quality of the signals has been established using the criteria of audibility and the levels of quantization used in the digitalizing process by the data acquisition equipment.

Two accelerometers have been used in the experiences. Both of them attached to the sound card of a portable computer. The first one is insect-detection oriented (SP-1L probe from AED-2000 instrument). The second one is the model KB12V (MMF); seismic accelerometer, consequently with a high sensitivity and a short band-with. One of the goals of this experiment consists of establishing insect identification criteria, independent from the sensor.

The paper is structured as follows: Section 2 summarizes the problem of acoustic detection of termites; Section 3 remembers the theoretical background of HOS, focussing on the computational tools employed. Experiments are drawn in Section 4; this section is intended for use as a tool for interpreting results from a HOS-based experiment. And finally, conclusions are explained in Section 5.

2. Acoustic detection of termites

2.1. Characteristics of the AE alarm signals

Acoustic emission (AE) is defined as the class of phenomena whereby transient elastic waves are generated by the rapid (and spontaneous) release of energy from a localized source or sources within a material, or the transient elastic wave(s) so generated (ASTM, F2174-02, E750-04, F914-03[2]). This energy travels through the material as a stress or strain wave and is typically detected using a piezoelectric transducer, which converts the surface displacement (vibrations) to an electrical signal [3,8,9].

Termites use a sophisticated system of vibratory long distance alarm. When disturbed in their nests, extended gallery systems, soldiers produce sophisticated vibratory signals by drumming their heads against the substratum [10]. The drumming signals consist of pulse trains which propagate through the substrate (mechanical vibrations), with pulse repetition rates (beats) in the range of 10–25 Hz, and with burst rates around 500–1000 ms, depending on the species [11]. Soldiers produce such vibratory signals in response to disturbance (1–2 nm by drumming themselves) by drumming their head against the substratum (head banging). Workers can perceive these vibrations, become alert and tend to escape [12]. The most probable sounds (default) consists of feeding and excavating.

Fig. 1 shows one of the impulses within a typical four-impulse burst (alarm signals) and its associated power spectrum. Significant drumming responses are produced over the range 200 Hz–10 kHz. It is in this interval where the spectral identification of the specie (*Reticulitermes Lucifugus*) is performed. The carrier frequency of the drumming signal is defined as the main spectral component, which keeps with longer attenuation time, and in this case is around 2600 Hz.

It is important to remark that the recording conditions of alarm signals are very favorable in most of the situations (even in urban zones where parasitic noise is present). This is due to the characteristic and the intensity of the sound of the bursts. For this reason we used an economical directional microphone to record the register; *Ariston CME6* model, with a sensitivity of 623 dB and a bandwidth of 100 Hz–8 kHz. The device was connected to the sound card of a portable computer, and the sample frequency was adjusted to 96,000 Hz.

The spectrum is not flat as a function of frequency, as one would expect for a pulse-like event. This is due to the frequency response of the sensor (its selective characteristics) and also to the frequency-dependent attenuation coefficient of the propagation media, wood and air.

Due to our identification purposes we are concerned of the spectral patterns of the signals; so we do not care about the energy levels. Besides, as a result of the higher-order processing, the original energy levels of the signals are lost, but not as the extent of the levels of parasitic noise which are coupled to the signals.

Furthermore, signals from feeding an excavating activities differ from alarm signals in the fact that the last ones have clear time patterns. But all of them come essentially from random impulse events that induce the same response of the sensor and the traversed media. The main handicap is the low

[2] American Society for Testing and Materials. F2174-02: Standard Practice for Verifying Acoustic Emission Sensor Response. E750-04: Standard Practice for Characterizing Acoustic Emission Instrumentation. F914-03: Standard Test Method for Acoustic Emission for Insulated and Non-Insulated Aerial Personnel Devices Without Supplemental Load Handling Attachments.

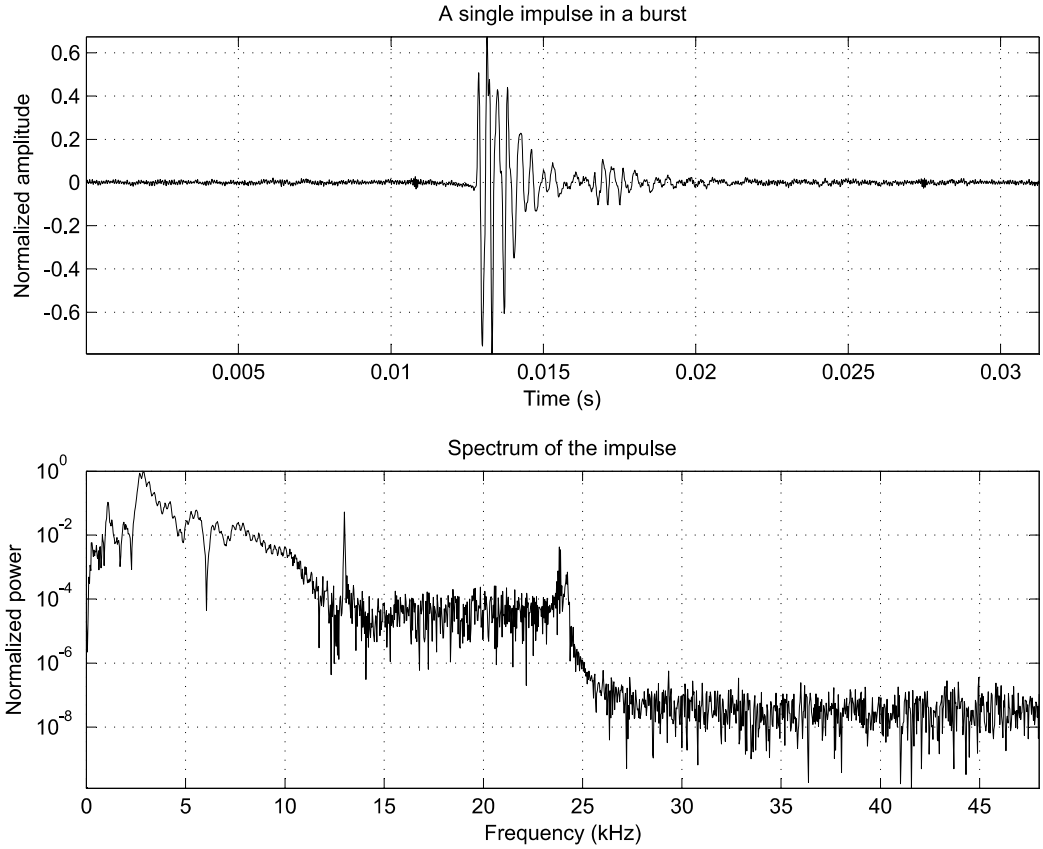

Fig. 1. A single pulse extracted from a four-pulse burst (top) and its associated power spectrum (bottom). Significant amplitudes are found up to 10 kHz. In the interval 10–27 kHz the activity remains constant in a lower energy level.

intensity of the involved levels. Herein after we are concerned of detecting normal (by default) activity of insects, which in fact are the key to earlier detection. We use accelerometers' recording comprising several levels of audibility. First, we classify the waveform of AE events.

2.2. AE types, devices, ranges of measurement and HOS techniques

Two ideal basic types of acoustic emissions are commonly distinguished according to their time instances. Continuous acoustic emission is the most difficult to characterize when several emissions coexist in the same time-series, interfering each other and, consequently making difficult the task of extracting useful information. This is for example the case of a sensor output buried in noise. When the measurand is the whole continuous sequence of AE signals, it is best measured as RMS.

Burst-type emission is best characterized by threshold crossing detection. The AE signal voltage is compared with an internally generated reference (threshold). Each time the signal crosses the threshold level, the detecting device emits a pulse (count) which is summed up by a processor, in the counting assembly. The total count is provided within a time interval (measurement time). When the instrument fails to detect a pulse within a specified timeout, the detector circuit turns off and stores the pulses in the measuring time as a hit.[3]

The former AE types are found in real situations in miscellaneous forms, with noise background. Spiky continuous noise characterizes turbulence in fluid or gas flow systems and voltage fluctuations in high tension lines. Characterization helps establish the quality of the energy flow.

Burst-type emission with continuous noise background can be observed in the following situations: cavitation phenomena in fluid flow systems, discharges in power transformers with core noise, sig-

[3] In the case of the widely used system AED-2000, the timeout period is called *hit determination time* and is 1 ms.

nals from leakage in flat-bottom storage tanks and machinery monitoring applications on bearings and gears.

Many efforts to develop techniques for detecting hidden termite infestations have produced only a few real alternatives to traditional visual inspection methods. Remarkable alternatives are ground-based monitoring devices and sensors that detect acoustic emissions of termites in wood (like AED-2000). It has been proved that nearly all noise signals have most of their energy below 20 kHz[4] [10,12]. Besides, termite activities in the wood generate a significant amount of acoustic emission with frequency components extending to above 100 kHz. Therefore, acoustic emission sensors are successful because they are non-destructive and operate at high frequency (>40 kHz) where background noise is negligible and does not interfere with insect sounds [13].

Soil and wood have a much longer coefficient of sound attenuation than air and the coefficient increases with frequency. This attenuation reduces the detection range of acoustic emission to 2–5 cm in soil and 2–3 m in wood, as long as the sensor is in the same piece of material [13]. The range of acoustic detection is much greater at frequencies <10 kHz, and low frequency accelerometers have been used to detect insect larvae over 1–2 m in grain and 10–30 cm in soil [1,13]. To sum up, acoustic measurement devices have been used primarily for detection of termites in wood (feeding and excavating), but there is also the need of detecting termites in trees and soil surrounding building perimeters.

It has been shown that the independent component analysis (ICA) success in separating termite emissions with small energy levels in comparison to the background noise. This is explained away by statistical independence basis of ICA, regardless of the energy associated to each frequency component in the spectra [4,14]. The same authors have proven that the diagonal bispectrum can be used as a tool for characterization purposes [5], using a set of synthetics comprising bursts and noise processes, previously designed and with a symmetrical probability density function. With the aim of facing the problem of detection from real activity signals we use the binomial bispectrum–trispectrum to extract frequency patterns. The guts of HOS and their associated polyspectra are exposed in Section 3.

[4] The sensor used was a model A3 resonant sensor (30–50 kHz) manufactured by Physical Acoustics, with a JFET low noise voltage amplifier, model 324-3.

3. Higher-order statistics (HOS)

3.1. Motivation of HOS

Gaussian processes are completely characterized by the autocorrelation sequence and its associated Fourier transform, the power spectrum. However, there are numerous cases where we have to look beyond the autocorrelation to extract information regarding deviations from Gaussianess and non-linear characterization.

Data sequences, and their associated power spectra, which have been obtained by multiplying more than two time-series are called higher-order statistics. They contain additional information regarding the phase of the signals involved in the quantities. This information is used with the objective of solving the problem described in the paragraph above.

The power spectrum (second order spectrum) is a particular case of higher-order spectra. The third order spectrum is called the *bispectrum* and the fourth-order spectrum is called the *trispectrum*. They are defined to be the Fourier transforms or the third- and fourth-order cumulant sequences, respectively.

Polyspectra consist of higher-order moment spectra and cumulant spectra and can be defined for both deterministic signals and random processes. Moment spectra can be very useful in the analysis of deterministic signals (transient and periodic), whereas cumulant spectra are of great importance in the analysis of stochastic signals.

The motivation of the polyspectral analysis yields in three applications: (a) To suppress Gaussian noise processes of unknown spectral characteristics; the bispectrum also suppress noise with symmetrical probability distribution, (b) to reconstruct the magnitude and phase response of systems, and (c) to detect and characterize non-linearities in time series.

In the following, we settle the mathematical foundations of HOS in order to improve the understanding of the graphs, and the subsequent characterization process.

3.2. Cumulants

High-order statistics, known as cumulants, are used to infer new properties about the data of non-Gaussian processes [15]. Before cumulants, such processes had to be treated as if they were Gaussian [16]. Cumulants and their associated Fourier transforms, known as polyspectra [17], reveal

information about amplitude and phase, whereas second-order statistics (power, variance, covariance and spectra) are phase-blind [18].

Before the definitions, it is convenient to remark that cumulants of order higher than 2 are all zero in signals with Gaussian probability density functions. What is the same, cumulants are blind to any kind of a Gaussian process. This is the reason why it is not possible to separate these signals using the statistical approach [16–18].

The relationship between the cumulant of r stochastic signals, $\{x_i\}_{i\in[1,r]}$, and their moments of order p, $p \leqslant r$, can be calculated by using the *Leonov–Shiryaev* formula [4,17,18]

$$\mathrm{Cum}(x_1,\ldots,x_r) = \sum(-1)^{p-1}\cdot(p-1)!\cdot E\left\{\prod_{i\in v_1} x_i\right\} \cdot E\left\{\prod_{j\in v_2} x_j\right\}\cdots E\left\{\prod_{k\in v_p} x_k\right\} \tag{1}$$

where the addition operator is extended over all the set of $v_i\,(1 \leqslant i \leqslant p \leqslant r)$ and v_i compose a partition of $1,\ldots,r$. By using (1) the second-, third-, and fourth-order cumulants, for a zero mean variable, are given by

$$\mathrm{Cum}(x_1,x_2) = E\{x_1\cdot x_2\} \tag{2a}$$

$$\mathrm{Cum}(x_1,x_2,x_3) = E\{x_1\cdot x_2\cdot x_3\} \tag{2b}$$

$$\begin{aligned}\mathrm{Cum}(x_1,x_2,x_3,x_4) &= E\{x_1\cdot x_2\cdot x_3\cdot x_4\}\\ &\quad - E\{x_1\cdot x_2\}E\{x_3\cdot x_4\}\\ &\quad - E\{x_1\cdot x_3\}E\{x_2\cdot x_4\}\\ &\quad - E\{x_1\cdot x_4\}E\{x_2\cdot x_3\}\end{aligned} \tag{2c}$$

In the case of non-zero mean variables x_i have to be replaced by $x_i - E\{x_i\}$.

Let $\{x(t)\}$ be a rth-order stationary random real-valued process. The rth-order cumulant is defined as the joint rth-order cumulant of the random variables $x(t), x(t+\tau_1),\ldots,x(t+\tau_{r-1})$,

$$\begin{aligned}&C_{r,x}(\tau_1,\tau_2,\ldots,\tau_{r-1})\\ &\quad = \mathrm{Cum}[x(t),x(t+\tau_1),\ldots,x(t+\tau_{r-1})]\end{aligned} \tag{3}$$

The second-, third- and fourth-order cumulants of zero-mean $x(t)$ can be expressed using (2) and (3)

$$C_{2,x}(\tau) = E\{x(t)\cdot x(t+\tau)\} \tag{4.a}$$

$$C_{3,x}(\tau_1,\tau_2) = E\{x(t)\cdot x(t+\tau_1)\cdot x(t+\tau_2)\} \tag{4.b}$$

$$\begin{aligned}C_{4,x}(\tau_1,\tau_2,\tau_3) &= E\{x(t)\cdot x(t+\tau_1)\cdot x(t+\tau_2)\cdot x(t+\tau_3)\}\\ &\quad - C_{2,x}(\tau_1)C_{2,x}(\tau_2-\tau_3)\\ &\quad - C_{2,x}(\tau_2)C_{2,x}(\tau_3-\tau_1)\\ &\quad - C_{2,x}(\tau_3)C_{2,x}(\tau_1-\tau_2)\end{aligned} \tag{4.c}$$

By putting $\tau_1=\tau_2=\tau_3=0$ in (4), we obtain

$$\gamma_{2,x} = E\{x^2(t)\} = C_{2,x}(0) \tag{5.a}$$

$$\gamma_{3,x} = E\{x^3(t)\} = C_{3,x}(0,0) \tag{5.b}$$

$$\gamma_{4,x} = E\{x^4(t)\} - 3(\gamma_{2,x})^2 = C_{4,x}(0,0,0) \tag{5.c}$$

Eq. (5) are measurements of the variance, skewness and kurtosis of the distribution in terms of cumulants at zero lags. Normalized kurtosis and skewness are defined as $\gamma_{4,x}/(\gamma_{2,x})^2$ and $\gamma_{3,x}/(\gamma_{2,x})^{3/2}$, respectively. We will use and refer to normalized quantities because they are shift and scale invariant. If $x(t)$ is symmetrically distributed, its skewness is necessarily zero (but not *vice versa*); if $x(t)$ is Gaussian distributed, its kurtosis is necessarily zero (but not *vice versa*).

In practice, the computation of the cumulants and polyspectra are based in estimates. For example in this paper, the fourth-order cumulant of a N-sample signal vector $x(n)$ is computed by means of a biased estimates via Eq. 6:

$$\begin{aligned}C_{4,x}(k,l,m) &= \mathrm{Cum}[x(n),x(n+k),x(n+l),x(n+m)]\\ &= \frac{1}{N}\sum_{n=0}^{N-1} x(n)\cdot x(n+k)^*\cdot x(n+l)^*\\ &\quad\cdot x(n+m)^* - \frac{1}{N^2}\left[\sum_{n=0}^{N-1} x(n)\cdot x(n+k)^*\right]\\ &\quad\times\left[\sum_{n=0}^{N-1} x(n+l)^*\cdot x(n+m)^*\right]\\ &\quad - \frac{1}{N^2}\left[\sum_{n=0}^{N-1} x(n)\cdot x(n+l)^*\right]\\ &\quad\times\left[\sum_{n=0}^{N-1} x(n+k)^*\cdot x(n+m)^*\right]\\ &\quad - \frac{1}{N^2}\left[\sum_{n=0}^{N-1} x(n)\cdot x(n+m)^*\right]\\ &\quad\times\left[\sum_{n=0}^{N-1} x(n+k)^*\cdot x(n+l)^*\right],\end{aligned} \tag{6}$$

where, $k,l,m\in[-\chi,\ldots,-1,0,1,\ldots,+\chi]$, and $n=0,1,\ldots,N-1$. χ is the maximum time shift (lag) between samples of a record.

3.3. Polyspectra

We will assume in the following that the cumulant sequences satisfies the bounding condition:

$$\sum_{\tau_1=-\infty}^{\tau_1=+\infty} \cdots \sum_{\tau_{r-1}=-\infty}^{\tau_{r-1}=+\infty} |C_{r,x}(\tau_1, \tau_2, \ldots, \tau_{r-1})| < \infty \qquad (7)$$

Under this assumption, the higher-order spectra are usually defined in terms of the rth-order cumulants as their $(r-1)$-dimensional Fourier transforms

$$S_{r,x}(f_1, f_2, \ldots, f_{r-1}) = \sum_{\tau_1=-\infty}^{\tau_1=+\infty} \cdots \sum_{\tau_{r-1}=-\infty}^{\tau_{r-1}=+\infty} C_{r,x}(\tau_1, \tau_2, \ldots, \tau_{r-1}) \cdot \exp[-\mathrm{j}2\pi(f_1\tau_1 + f_2\tau_2 + \cdots + f_{r-1}\tau_{r-1})] \qquad (8)$$

The special poly-spectra derived from (8) are power spectrum ($r = 2$), bi-spectrum ($r = 3$) and tri-spectrum ($r = 4$). Only power spectrum is real, the others are complex magnitudes.

Polyspectra are multidimensional functions which comprise a lot of information. As a consequence, their computation may be impractical in some cases [19]. To extract useful information one-dimensional slices of cumulant sequences and spectra, and bi-frequency planes are employed in non-Gaussian stationary processes [5].

Having settled down the motivation of the experiment, hereinafter we present que results obtained by means of the tools described here.

4. Experimental results

4.1. Pre-processing and bispectrum of data sequences from the AED-2000 probe

The strategy of the experiment has the main goal of trying to clarify if a non-suited accelerometer, or vibratory sensor, can be used instead of an insect-detection oriented (*ad hoc*) transducer, in a noisy scenario. We use the sound card of a portable computer with the aim of reducing the data acquisition cost of the equipment.

The data acquisition stage took place in a residential area of the "Costa del Sol" (Málaga—

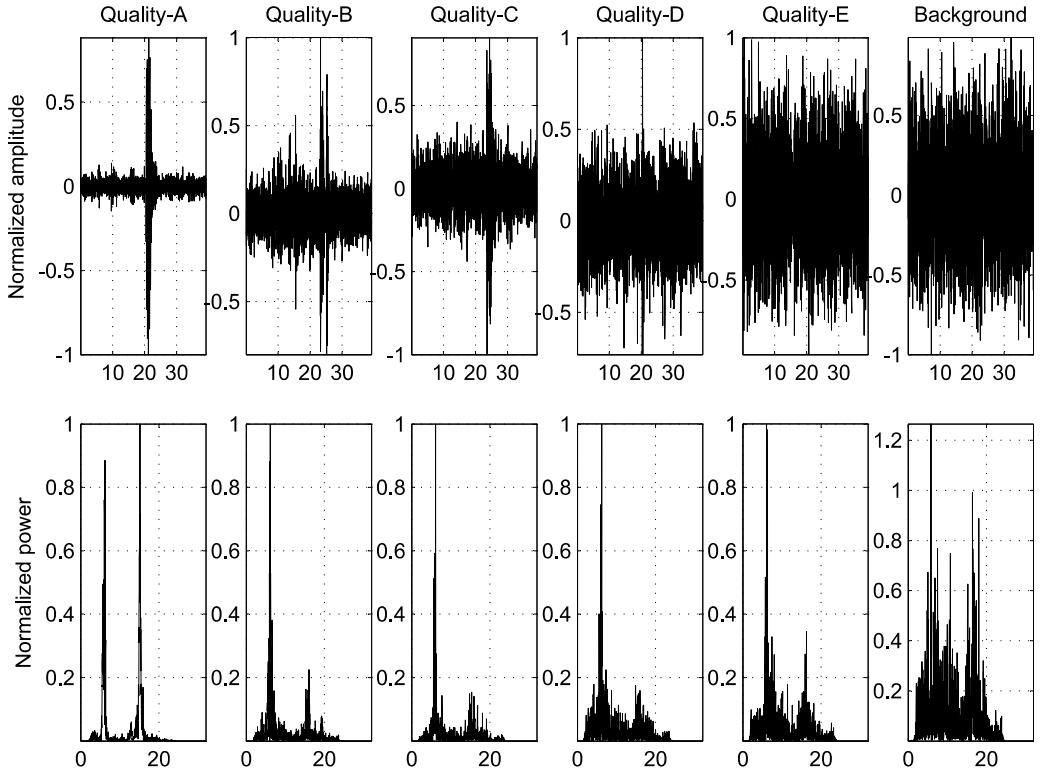

Fig. 2. Average power spectra of six categories of emissions in comparison to the background. The first row of graphs contains one signal of each quality type. The sampling frequency was 64 kHz. Abscissae of time sequences (ms); abscissae of spectra (kHz).

Spain), at the beginning of the reproductive season of the termites. The sensors were attached (plunged) in the soil surrounding affected trees (above the roots). We worked under the hypothesis of having a 500 m-radius of an affected circular perimeter.

The probe SP-1L from the equipment AED-2000 has been taken as the reference for a twofold purpose. First, we analyze the power spectra of signals with different qualities, to decide whether it is possible to use second-order spectra for identification purposes. Secondly, we settle down a higher-order detection criterium in the frequency domain, which in turn is used with the second accelerometer, the model KB12V (seismic accelerometer). Each graph is the result of averaging 15 2500-sample registers from *R. Lucifugus* feeding activity. Fig. 2 shows the average power spectra of six signal categories according to their amplitude quantization levels. These AE signals were acquired by the sensor SP-1L, using a sampling frequency of 64 kHz and a resolution of 16 bits. These spectra are compared to the background in order to establish an identification criterium. Vibrations of qualities *D* and *E* are inaudible.

Quality-A (Q-A) signals' amplitudes belong to the quantization levels interval [25,000, 30,000]. Q-B levels are in [15,000, 20,000]. Q-C levels are in [10,000, 15,000]. Quality-D levels are in the interval [5000, 10,000]. Finally, Q-E impulses are completely buried in the background. We are sure about the infestation, so the AE events in these series are due to termite activity, probably in the perimeter of the measurement.

The two main frequency components in the spectra of Fig. 2 appear at 6 and 15 kHz, respectively, which are associated to the frequency response of the sensor, to the features of the sounds produced by the specie of termite and to the characteristics of the substratum, where the emissions propagate. We conclude that using the probe SP-1L we can detect an infestation by interpreting the power spectra diagrams. This is due to the difference that the

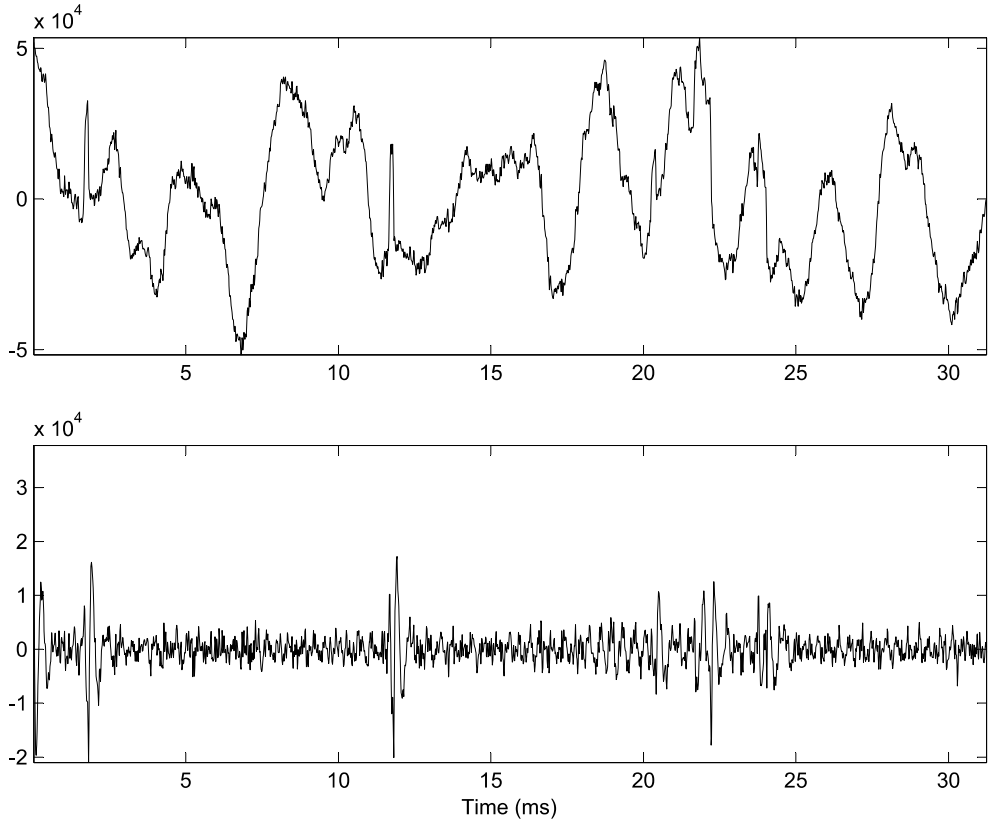

Fig. 3. A signal from KB12V accelerometer. The low frequency components mask the AE events associated to the emissions (top). Once the signal has been filtered the low-level impulses arise (bottom).

emissions exhibit in comparison to the flatter shape of the background spectra (sixth column of graphs in Fig. 2).

It is remarkable that we use the sensors beyond their band-width limit, specified by the manufacturer. Sensor included with AED-2000 is not characterized and the MMF-accelerometer KB12V has a bandwidth of 100 Hz. The complete frequency response of these transducers had to be obtained before the experiment. We take advantage from their high sensitivity.

Signals have been previously high-pass filtered in order to suppress low frequency components which would mask the higher-frequency components. A fifth-order *Butterworth* digital filter with cut-off frequency of 2 kHz is used. To show the effect of filtering we include Fig. 3.

The impulses resulting from the filter action constitute the *fingerprints* of the AE signals, associated to feeding and excavating activities of termites.

The calculation of higher-order spectra is performed with a twofold purpose. The first objective consists of enhancing the detection criteria in the frequency domain. Secondly, with the purpose of using more economic sensors, with a lower sensitivity and a higher band-width. Fig. 4 shows the average diagonal bispectra associated to the signals acquired with the probe SP-1L. It was chosen a maximum lag $\chi = 512$ to compute the third-order auto-cumulants of the signals. The bottom bispectrum characterizes the background sound (the most unfavourable, with an amplitude of four-orders of magnitude less than Q-A).

The main frequency component in Fig. 4 let us establish a detection criterium based in the identification of this maximum value. It is remarkable that this frequency is also associated to the sensor. Another sensor would carry another bispectrum shape. For that reason, the proposed method of insect detection is based in the previous characterization of the transducer. On the other hand, the magnitudes of the bispectra in Fig. 4 do not suffer a dramatic attenuation from high to low levels (two orders from Q-A to Q-E). This fact reinforces

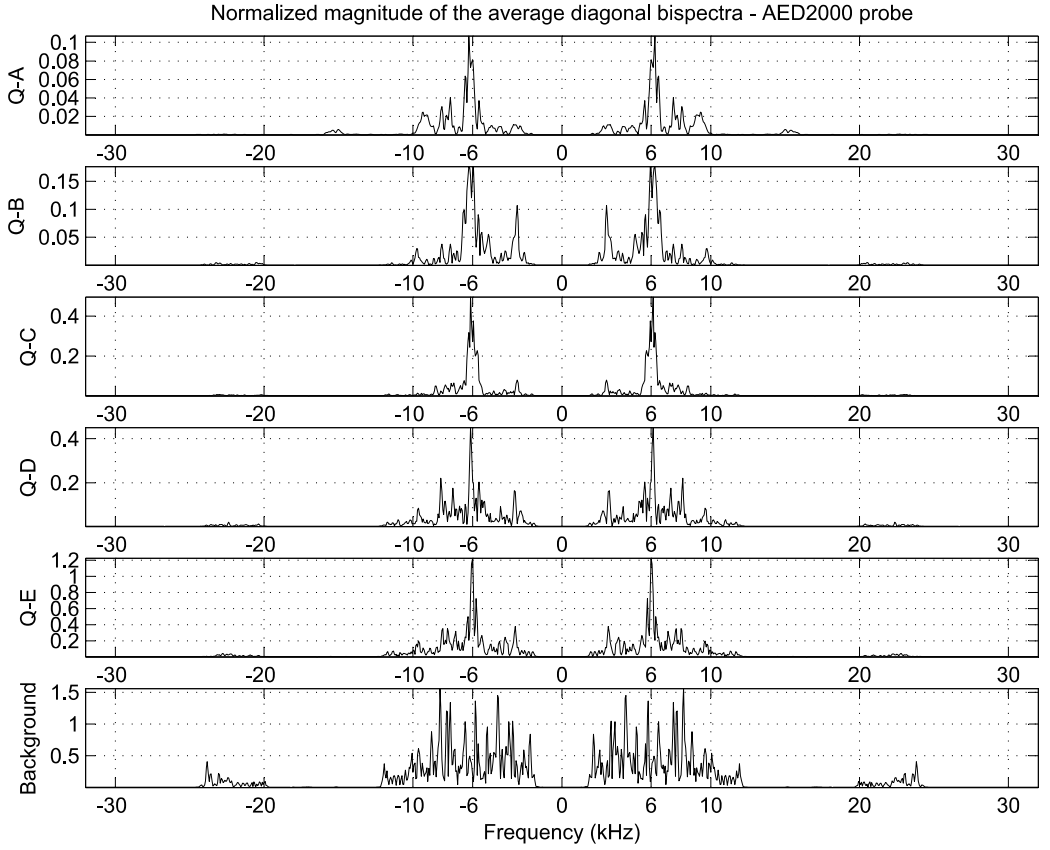

Fig. 4. Average diagonal bispectra of raw signals acquired by the probe SP-1L from AED-2000 in comparison to the background sounds, for a maximum lag, $\chi = 512$. Each bispectrum results from averaging 15 2500-data registers.

the criterium of identification, in the sense that it is the noise (symmetrically distributed) which is mainly reduced in the higher-order computation. In the next subsection we use the seismic vibratory sensor to confirm this experience.

4.2. Bispectrum analysis of data sequences from the KB12V accelerometer

The seismic accelerometer was characterized in a former work [4], and it was found a resonance frequency of 2600 Hz. In Fig. 3 it was remarked the importance of applying the high-pass filter in order to enhance the hidden impulses, buried in the low frequency components. This in fact easies the use of the accelerometer KB12V, which has a maximum operative range of 25 kHz (over the band-width limit).

The ultrasonic AE sensors used in former works (like one in [1]) do not face neither the problem of low-frequency effects (couplings or bias currents from the sensor), nor the effects of colored noise in the audio band. Filtering avoid the first drawback, and HOS reduces effects of symmetrically distributed noise.

Fig. 5 shows the difficulties we faced when trying to identify or detect the emissions using the transducer MMF-KB12V (seismic accelerometer). The spectra (the symmetric version) in the middle graph of Fig. 5 does not present a distinctive shape as the ones in Fig. 2. In fact, the background random impulses produce the same shape in the spectrum (power spectrum). Moreover, the sound levels produced by the noise and the insects have the same magnitude orders when the distance between the transducer and the source increases. Probably this can be explained out from the design strategy of the equipment AED-2000 and its probe, which filters (attenuates) the low-frequency audio signals. We have to take advantage from the higher-order spectra.

In the bottom graph of Fig. 5 the main frequency component appears near 2600 Hz in the diagonal bispectrum. At a first glance the shapes of second-order and third-order spectra are very similar. But

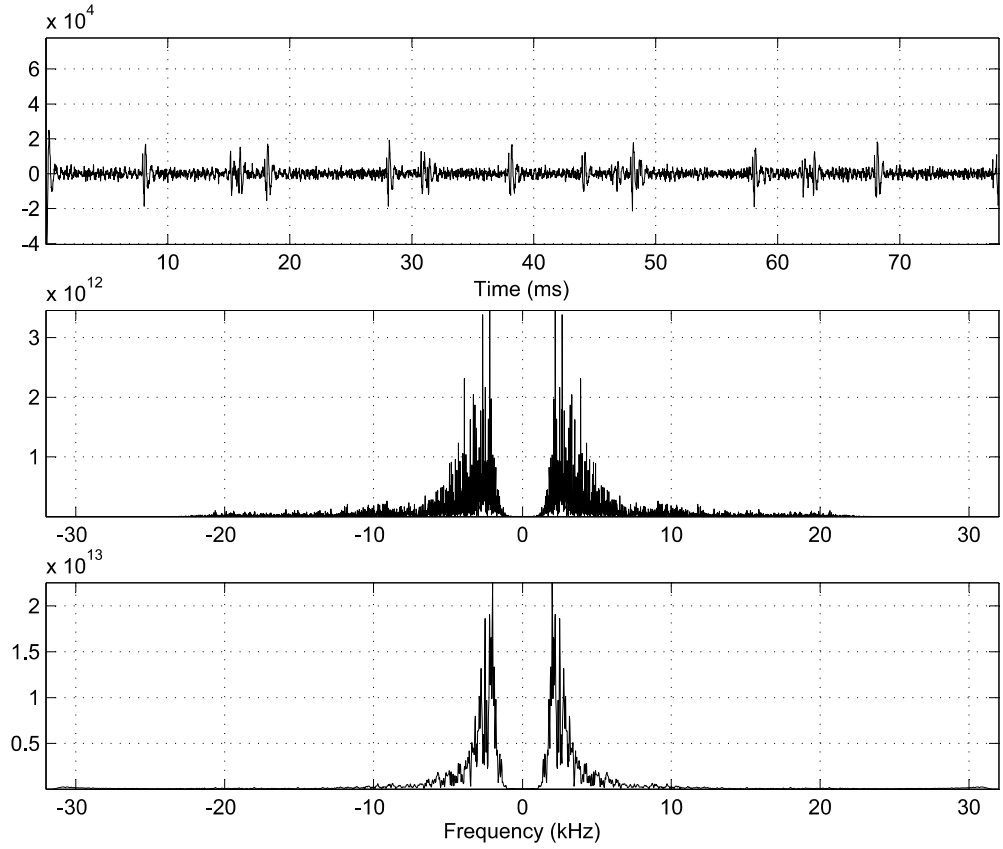

Fig. 5. From top to bottom: A sequence of filtered impulses from the sensor KB12V, the symmetric power spectrum and its associated bispectrum, for a maximum lag, $\chi = 1024$.

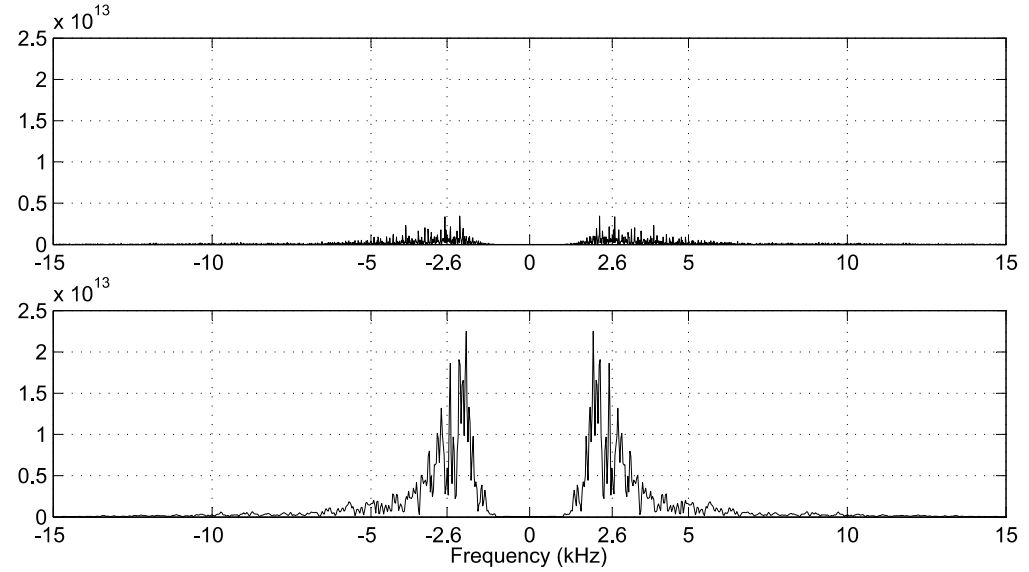

Fig. 6. Second and third-order spectra (for a maximum lag, $\chi = 1024$) of the seismic accelerometer recordings. Units are based in the number of quantization levels 2^{16}.

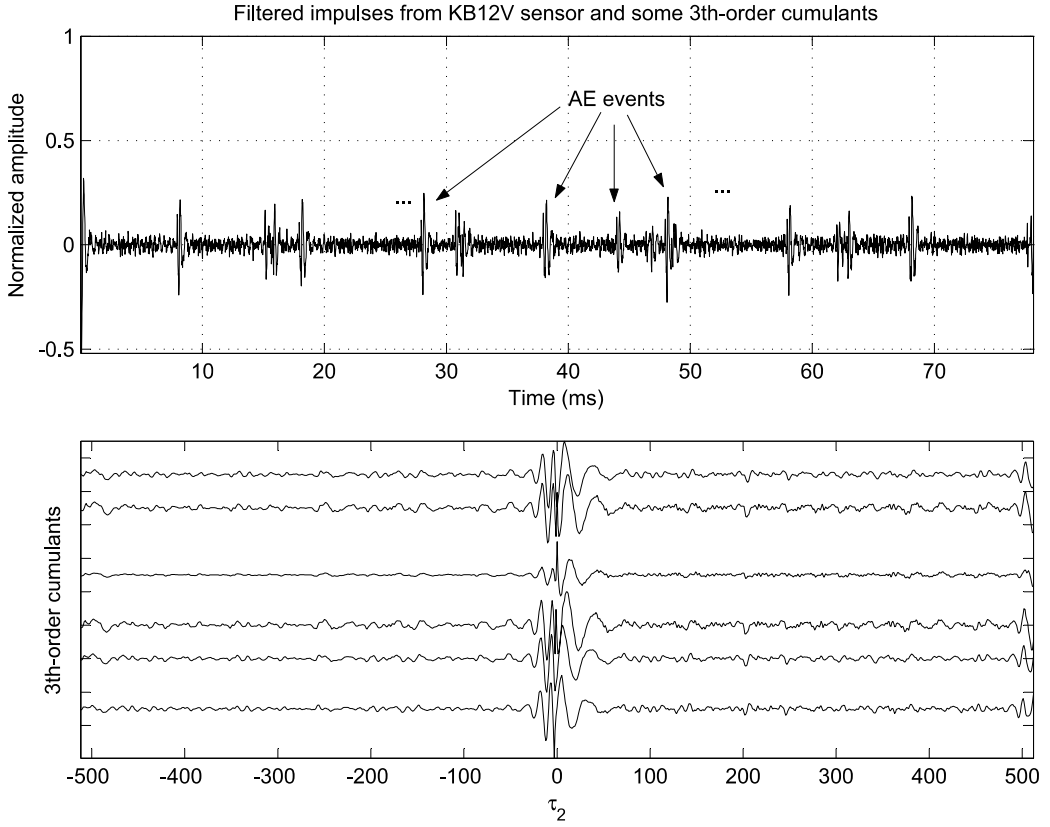

Fig. 7. A sequence of AE events (upper graph) and some third-order cumulants; from bottom to top $\tau_1 = -2, -1, 0, 1, 2, 3$, for a maximum lag, $\chi = 512$; $\tau_2 \in [-\chi, \chi]$.

a thorough examination of the bispectrum reveals important details. The bispectrum's shape is more accused and the frequency contents up to 2600 Hz are clearly enhanced over the rest of the frequency components. The former remark is confirmed in the graphs depicted in Fig. 6, where both graphs are drawn using the same scale.

To examine the time instances of the third-order cumulants we have included some autocumulants in the surrounding of zero-lag, in Fig. 7. For a fixed value of τ_1, the complete sequence of impulses is transformed into a single impulse (or transient) in the neighborhood of the considered lag.

The lag (τ) is the time-offset of signal samples. For example, a sequence of waveform measurements 1-2000 with a lag =1 will compare data 1-1999 to samples 2-2000 ; a lag =2 compares samples 1-1998 to samples 3-2000; etc.

As we can see from Fig. 7, cumulants represent the *fingerprints* of the emissions. In fact the cumulant sequence can be seen as a perturbation propagating from low to high values of the lag time.

These results support the idea of a frequency-based identification criterium. In the next section we try to enhance the procedure by means of the diagonal trispectrum.

4.3. Fourth-order analysis

Fourth-order non-zero-lag auto-cumulants of the acquired waveforms and the associated spectra (trispectra) are depicted and analyzed in this subsection to complement the characterization of the signal.

We used fourth-order cumulant slices through possible combinations of lag triplets. The slices are well-suited to signal characterization and classification. The higher-order statistical structure of the cubic-3D fourth-order cumulant matrix array (the tensor of data) have been previously examined to select a proper slice. Following the same guidelines of the third-order version, we try to find the "fingerprint" of the acquired signal.

Fig. 8 shows the selected slice from the cubic-3D data arrangement to perform the trispectral analysis. A maximum lag of $\chi = 100$ has been selected for the sake of reducing the computational time because we do not gain substantially in resolution with a higher value of χ.

From Fig. 8 it is clear that the diagonal slice would be useful to settle down an axis through begin the analysis. But we have adopted a more general criterium, selecting the diagonal of the 3D-cubic structure as the information axis.

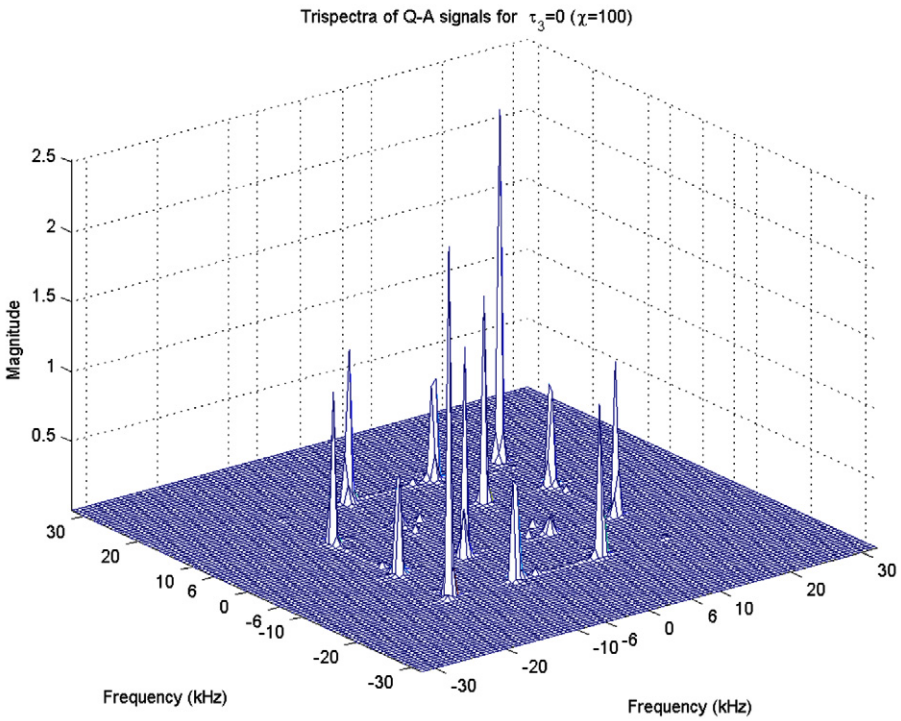

Fig. 8. The slice of the trispectrum corresponding to $\tau_3 = 0$, for a Q-A type signal.

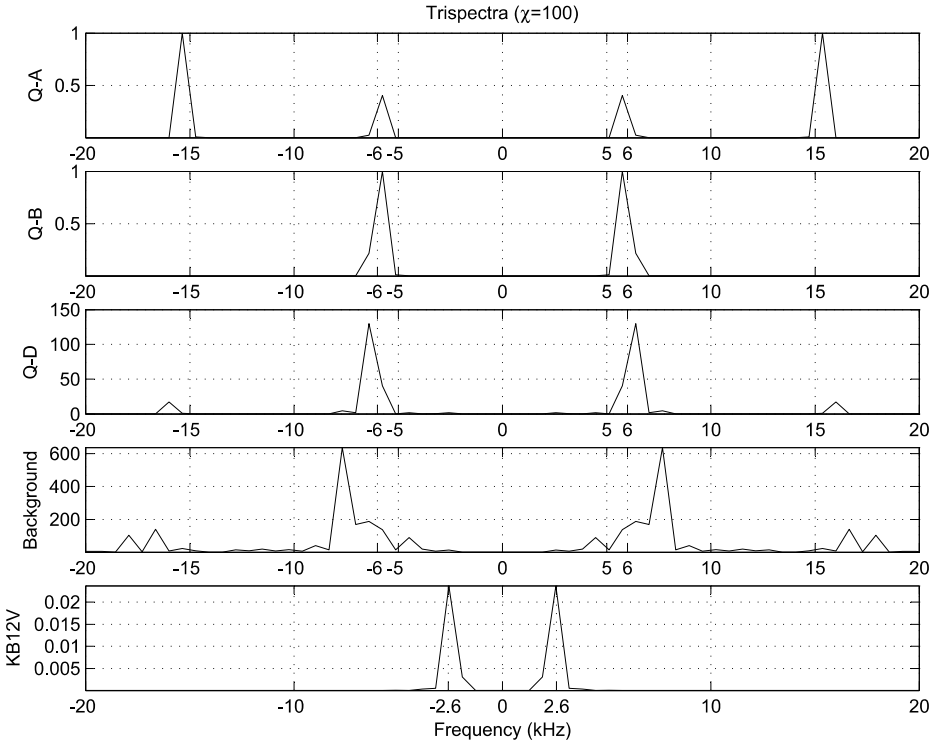

Fig. 9. The slice of the average trispectrum corresponding to the diagonal of the cubic structure, for different types of waveform. From top to bottom: Q-A–B–D from SP-1L probe, the trispectrum of the background and the trispectrum of signals acquired by the accelerometer KB12V.

Fig. 9 shows the average diagonal trispectra corresponding to different signals, which have been acquired with both accelerometers, in comparison to the background diagonal trispectrum.

The presence of the peak in the boundaries of the frequency 6 kHz let us confirm the feasibility of the frequency-based identification criterium. The most disadvantageous diagonal trispectrum of the background (the fourth diagram in Fig. 9 from top to bottom) is more irregular and is centered in a different frequency component. Finally, the shape of the average trispectrum from the KB12V accelerometer reveals an abrupt region in the boundaries of its resonance frequency, 2.6 kHz.

On the basis of these results we establish the conclusions related to the identification criterium proposed.

5. Conclusions

In this work it has been shown that the bispectrum and the trispectrum (the diagonal slices) are valid tools for obtaining a decision criterium to distinguish a possible infestation, based in the feeding activities of the termites. We found this conclusion in three arguments.

First, higher-order cumulants and spectra, as defined herein, enable the signal analysis procedure to have access to waveform shape information that is typically unavailable when using prior-art (second-order) methods. In particular we remark the capability of enhancing the outline of the frequency diagrams. This is due to the rejection action exerted over symmetrically distributed noise processes. In fact, non-Gaussian processes are completely characterized by means of HOS.

Secondly, the potentially valuable information contained in an AE signal (most part of its spectrum) is related to the impulses. The average spectrum reveals amplitude information (the resonance peaks) but phase information is not shown. Higher-order spectra are arrangements of complex numbers and contain this additional information which can be valuable in a pattern recognition or identification criterium context.

Finally, it has been proven that using different sensors the criterium changes the frequency *set-*

point. The probability of a false alarm is very low, considering the fact that we had to provide, intentionally, the worst case of background noise. We have estimated this probability in a 1%.

Future work is focussed on reducing the computational complexity of HOS in two directions. By one side we are using compact functions, like FFT and FFTshift. Secondly, we have to adopt a compromise between the maximum lag (χ) and the resolution in order to save storage memory and time. These actions are oriented in the direction of implementing the algorithms in a digital signal processor, in an autonomous hand-held instrument.

Acknowledgements

The authors would like to thank the *Spanish Ministry of Education and Science* for funding the project DPI2003-00878, where the different noise processes have been modelled and contrasted; and also for supporting the PETRI project 95-0824-OP with the company *Contraplagas Ambiental S.L.* Our last thanks to the Andalusian Government for supporting the project TIC155, which involves HOS.

References

[1] W.P. Robbins, R.K. Mueller, T. Schaal, T. Ebeling, Characteristics of acoustic emission signals generated by termite activity in wood, in: Proceedings of the IEEE Ultrasonic Symposium, 1991, pp. 1047–1051.

[2] R.W. Mankin, J.R. Fisher, Current and potential uses of acoustic systems for detection of soil insects infestations, in: Proceedings of the Fourth Symposium on Agroacoustic, 2002, pp. 152–158.

[3] J.J.G. de la Rosa, C.G. Puntonet, I. Lloret, J.M. Górriz, Wavelets and wavelet packets applied to termite detection, in: Computational Science – ICCS 2005: 5th International Conference, GA, Atlanta, USA, 22–25 May 2005, Proceedings, Part I, Lecture Notes in Computer Science (LNCS), vol. 3514, 2005, pp. 900–907.

[4] J.J.G. de la Rosa, C.G. Puntonet, I. Lloret, An application of the independent component analysis to monitor acoustic emission signals generated by termite activity in wood, Measurement 37 (1) (2005) 63–76. Available online 12 October 2004.

[5] J.J.G. de la Rosa, I. Lloret, C.G. Puntonet, J.M. Górriz, Higher-order statistics to detect and characterise termite emissions, Electronics Letters 40 (20) (2004) 1316–1317, Ultrasonics.

[6] R. Miralles, L. Vergara, J. Gosalbez, Material grain noise analysis by using higher-order statistics, Signal Processing 84 (1) (2004) 197–205.

[7] A. Iturrospe, D. Dornfeld, V. Atxa, J.M. Abete, Bicepstrum based blind identification of the acoustic emission (AE) signal in precision turning, Mechanical Systems and Signal Processing 19 (1) (2005) 447–466.

[8] R. Piotrkowski, M.I.L. Pumarega, M. Armeite, J. Mieza, J.E. Ruzzante, Analysis of echoes in acoustic emission signals, in: 3rd Pan American Conference for Non-destructive Testing. Proceedings, vol. 1, j.e. ruzzante Edition, Rio de Janeiro-Brazil, 2003.

[9] R. Piotrkowski, A. Gallego, E. Castro, M. García-Hernández, J. Ruzzante, Ti and Cr nitride coating/steel adherence assessed by acoustic emission wavelet analysis, Non Destructive Testing and Evaluation (NDT and E) International 8 (4) (2005) 260–267.

[10] A. Röhrig, W.H. Kirchner, R.H. Leuthold, Vibrational alarm communication in the African fungus-growing termite genus macrotermes (isoptera, termitidae), Insectes Sociaux 46 (1999) 71–77.

[11] S. Connétable, A. Robert, F. Bouffault, C. Bordereau, Vibratory alarm signals in two sympatric higher termite species: Pseudacantotermes spiniger and p. militaris (termitidae, macrotermitinae), Journal of Insect Behaviour 12 (3) (1999) 90–101.

[12] J. Reinhard, J.-L. Clément, Reaction of European reticulitermes termites to soldier head capsule volatiles (isoptera, rhinotermitidae), Journal of Insect Behaviour 15 (1) (2002) 95–107.

[13] R.W. Mankin, W.L. Osbrink, F.M. Oi, J.B. Anderson, Acoustic detection of termite infestations in urban trees, Journal of Economic Entomology 95 (5) (2002) 981–988.

[14] J.J.G. dela Rosa, C.G. Puntonet, J.M. Górriz, I. Lloret, An application of ICA to identify vibratory low-level signals generated by termites, in: Proceedings of the Fifth International Conference, ICA 2004, Granada, Spain, Lecture Notes in Computer Science (LNCS), vol. 3195, 2004, pp. 1126–1133.

[15] M.J. Hinich, Detecting a transient signal by bispectral analysis, IEEE Transactions on Acoustics 38 (9) (1990) 1277–1283.

[16] A. Swami, J.M. Mendel, C.L. Nikias, Higher-Order Spectral Analysis Toolbox User's Guide, 2001.

[17] C.L. Nykias, J.M. Mendel, Signal processing with higher-order spectra, IEEE Signal Processing Magazine (1993) 10–37.

[18] J.M. Mendel, Tutorial on higher-order statistics (spectra) in signal processing and system theory: theoretical results and some applications, Proceedings of the IEEE 79 (3) (1991) 278–305.

[19] J. Jakubowski, K. Kwiatos, A. Chwaleba, S. Osowski, Higher order statistics and neural network for tremor recognition, IEEE Transactions on Biomedical Engineering 49 (2) (2002) 152–159.